

Technical Report 23

**MMT SEVENTH MIRROR FINAL TEST REPORT**

David S. Anderson

Prepared for  
The MMT Observatory

**MMT SEVENTH MIRROR FINAL TEST REPORT**

*David S. Anderson*

Optical Sciences Center  
University of Arizona  
Tucson, Arizona 85721

January 30, 1988

## INTRODUCTION

This report presents the final test data for the seventh Multiple Mirror Telescope (MMT7) mirror, along with an analysis of the data and the methods used to evaluate the mirror relative to the original design specifications. There are three categories of specifications that will be addressed: the radius of curvature, the figure quality, and the centration of the optical axis. A separate section of the report is devoted to each, along with two appendices that contain details of the phase measurement technique that was used to evaluate both the mirror surface and the centration of the optical axis. The measurement techniques developed for this mirror proved to be extremely reliable and accurate performed in the high environmental quality of the OSC shop, and will certainly advance the art of fabricating large optical surfaces.

## RADIUS OF CURVATURE

MMT7 was specified to be a parabola having an edge radius of  $9917.6 \pm 4$  mm. The setup for measurement of the edge radius is diagrammed in Figure 1. A knife edge was made to be coincident with a white-light point source. The position of the knife and source were adjusted along the optical axis to lie at the center of curvature of the edge zone. This position was repeatable to  $\pm 0.02$  mm. The distance between the edge of the mirror and the knife edge was measured with a steel tape and was found to be 9920.3 mm. Repeated trials of this measurement between two observers indicates a measurement error of  $\pm 0.5$  mm.

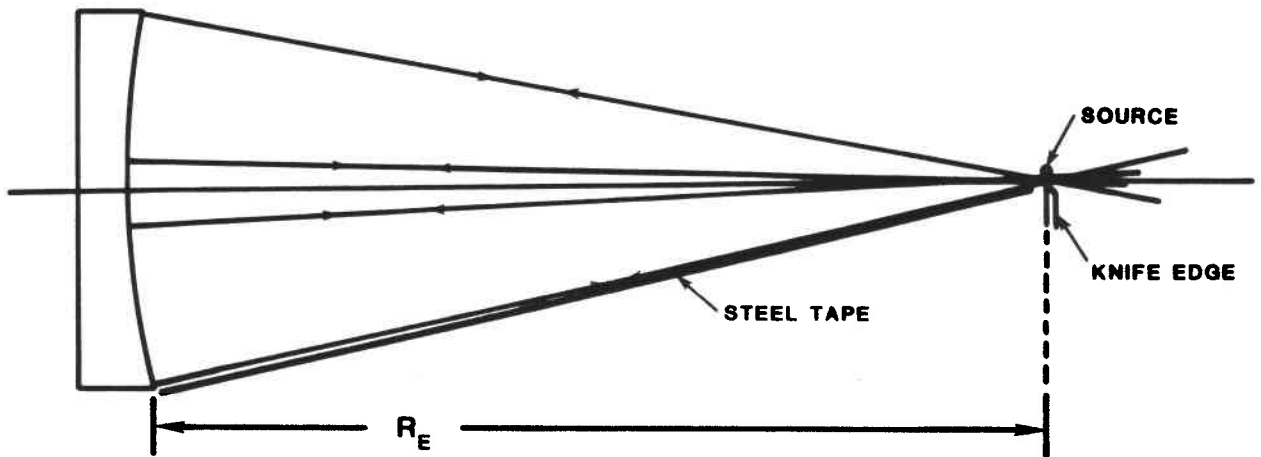


Figure 1. Setup for the measurement of the edge radius of curvature.

#### FIGURE QUALITY

The specifications for figure quality were as follows: rms surface irregularities between randomly selected pairs of points  $x$  cm apart on the mirrors surface to be less than or equal to:

0.013 wave	for $x = 4$ cm
0.024 wave	for $x = 8$ cm
0.043 wave	for $x = 16$ cm
0.077 wave	for $x = 32$ cm
0.105 wave	for $x = 64$ cm

where the wavelength used is 633 nm and where the wavefront disturbances on reflection are twice the values above. The pairs of points should be selectable at random on any part of the mirror surface, excluding the outer 0.5 in. of the edge and the central 10-in. diameter circle. The outer 0.5-in. edge should not depart from the true surface by more than  $1/2$  wave.

Phase measuring interferometry was used to evaluate the figure during the final figuring and testing sequence of fabrication. Details regarding the interferometer can be found in Appendix A. The primary rationale for this approach is the very high

spatial and high phase resolutions easily achievable with this method. High resolutions in both regimes are required for accurate evaluation of the surface in terms of these specifications. Appendix B is a prior report that describes details of the computational method used to evaluate the rms surface height differences from the phase data. Figure 2 is a plot of the rms difference values calculated from the phase data as the final figuring progressed. The convergence was quite rapid with, as expected, the longer spatial frequency differences meeting the specifications early in the process. The short spatial frequency difference specifications were arrived at more slowly because of the problem of keeping the aspheric figure sufficiently smooth. By the time all specifications were met, the long spatial frequencies were considerably better than called for in the specifications.

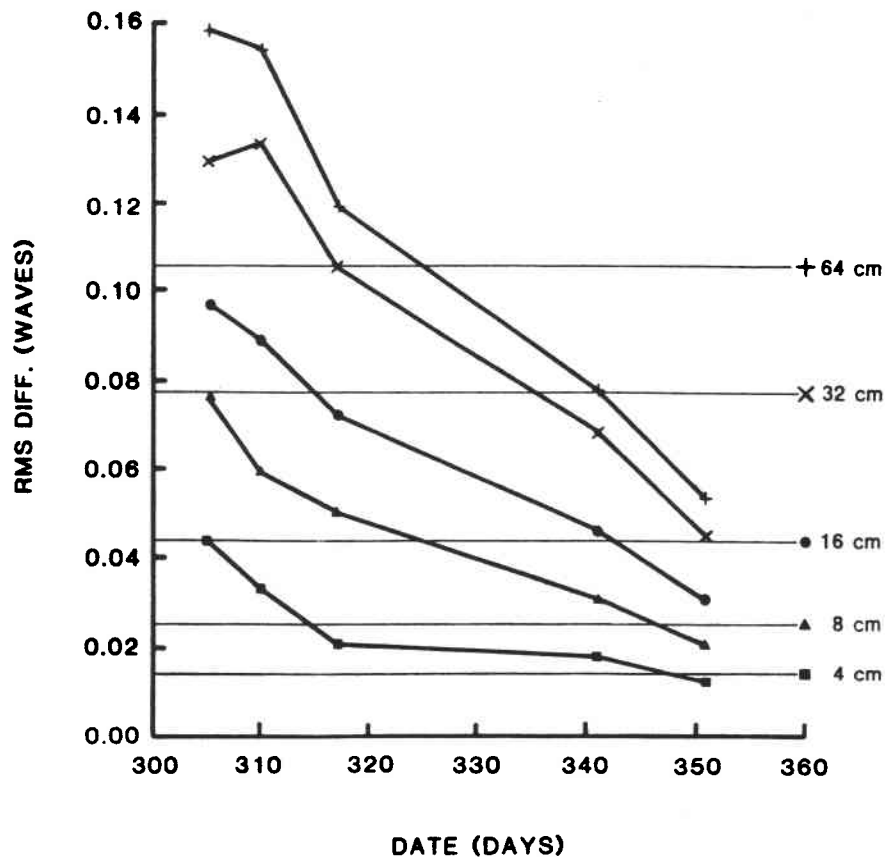


Figure 2. RMS difference versus number of days during final figuring. The horizontal lines are the specification values.

Test results indicated that the mirror met all specifications on December 16, 1987. Data from two tests made on December 17, 1987 and on January 4, 1988 were averaged to yield the best estimate of the surface quality in terms of the rms height differences. Both tests independently met the specifications and the repeatability indicates the stability and accuracy of the measurement. These results are shown in Table 1.

Table 1. RMS surface height differences.

Separation	Spec.	12/17/87	1/4/88	Average
4 cm	0.013	0.0126	0.0122	0.0124
8 cm	0.024	0.0211	0.0199	0.0205
16 cm	0.043	0.0311	0.0295	0.0303
32 cm	0.077	0.0458	0.0442	0.0450
64 cm	0.105	0.0538	0.0524	0.0531

Shown in Figures 3 and 4 are phase maps of the final test (1/4/88) in both a gray-scale format and a contour-map format. Figures 5 and 6 are interferograms of the surface with a 10 in. mask in the center and a 0.5 in. mask at the edge, which define the clear aperture over which the rms values were calculated.

Fitting a set of 24 Zernike polynomials to the phase data gives some insight into the character of the final surface. Table 2 lists the Zernike coefficients of the 24 polynomials listed in Appendix B, along with, in Table 3, a calculation of residuals and the Seidel aberrations. Note that astigmatism dominates the error, but, as shown in Appendix B, this type of error does not have a significant impact on the rms differences. The next most significant errors are those caused by the support structure, as can be seen most clearly in Figures 7 and 8 where the astigmatism (based on the Zernike fit) has been removed. The transparency showing the location of the hard points relative to the mirror can be overlaid on these maps. Note the pronounced drop-off at the edge outside and the raised area inside each hard point. Note also that the load is not perfectly symmetrical at the three hard points. The

deflection from the high area near the hard points to the low edge is approximately 0.12  $\lambda$  peak to peak (p-p).

**Table 2.** Zernike polynomial coefficients for different polynomial orders.

Term	N	rms fit	Zernike Polynomial Coefficients						
Plane	2	0.077	0.000	-0.001					
Sphere	3	0.077	0.000	-0.001	-0.001				
4th Order	8	0.051	-0.001	-0.001	0.001	0.053	0.039	-0.001	
			-0.002	-0.023					
6th Order	15	0.037	-0.000	-0.001	0.002	0.053	0.038	-0.001	
			-0.002	-0.025	-0.012	-0.038	0.016	0.003	
8th Order	24	0.032	-0.000	-0.001	0.002	0.053	0.032	-0.001	
			-0.002	-0.024	-0.013	-0.038	0.016	0.004	
			-0.014	-0.017	0.014	-0.007	-0.014	-0.015	
			-0.000	-0.021	0.003	0.004	0.018	-0.001	

**Table 3.** Seidel aberration coefficients and residuals.

	Magnitude (waves)	Angle (degs.)	Aberration		
	0.132	18.4	ASTIGMATISM		
	0.007	-122.4	COMA		
	-0.141		SPHERICAL		
No. of Points	Peak	Valley	P-V	rms	Strehl Ratio
29,316	0.121	-0.139	0.260	0.038	0.944

Figures 9 and 10 are slope maps of the surface reduced from the phase data with the astigmatism removed to show more clearly the remaining high-frequency errors. Note the print-through, evident both here and in the phase maps, which is  $<1/100$  wave p-p. The dominant errors are at the edge and center where the edge is asymmetrical for reasons which are unclear but are probably mount related. The center has a slight depression about 0.1 wave deep, extending out from the mask by about 1 in. There are very small residual zonal errors at about the 50% zone approximately  $1/40$  wave p-p, however the third-order spherical aberration is corrected to better than  $0.05 \lambda$  p-p.

Figure 11 is an interferogram of the surface with the 0.5-in. edge mask removed. From inspection of this interferogram it can be seen that the edge meets and indeed is much better than the  $1/2$  wave specification.

#### DETERMINATION OF THE OPTICAL AXIS POSITION

When the mirror is rotated about its mechanical center while under test from the center of curvature, the coma can be seen to increase and then decrease back to its original value when the mirror returns to its original position. This is an indication of coma in the mirror caused either by the support system or the optical axis not coinciding with the mechanical axis. Tests were performed that showed that the coma is most probably due to a decentration of the optical axis.

The relationship between the amount of decenter of the optical axis and the amount of coma it introduces in the wavefront can, for small decentrations, be determined by differentiating the third-order spherical aberration term; i.e.,

$$Z_4^0 = \frac{r^4}{8R^3}$$

$$\Delta Z_4^0 = \frac{r^3}{2R^3} \Delta r$$

where  $r$  is the aperture radius, which for this mirror is 914 mm,  $R$  is the radius of curvature which is 9920 mm, and  $\Delta r$  is the amount of decentration of the optical